

Post-buckling Response in Composite Plates under End-shortening Strain using Chebyshev Techniques

S.A.M. Ghannadpour^{1*} and M. Barekati²

1,2. New Technology and Engineering, Department, Shahid Beheshti University, G.C

*Postal Code: 1983963113, Tehran, IRAN

a_ghannadpour@sbu.ac.ir

In this paper, a method based on Chebyshev polynomials is developed for examination of geometrically nonlinear behavior of thin rectangular composite laminated plates under end-shortening strain. Different boundary conditions and lay-up configurations are investigated and classical laminated plate theory is used for developing the equilibrium equations. The equilibrium equations are solved directly by substituting the displacement fields with equivalent finite double Chebyshev polynomials. Using this method allows one to analyze the composite laminated plates with a combination of different boundary conditions on all edges. The final nonlinear system of equations is obtained by discretizing both equilibrium equations and boundary conditions with finite Chebyshev polynomials. Nonlinear terms created as the product of variables are linearized by using quadratic extrapolation technique to solve the system of equations. Since the number of equations is always more than the number of unknown parameters, the least squares technique is used to solve the system of equations. Some results for angle-ply and cross-ply composite plates with different boundary conditions are computed and compared with those available in the literature, wherever possible.

Keywords: Post-buckling, Chebyshev polynomials, End-shortening, Composite plates, Least squares technique, Quadratic extrapolation

Introduction

Composite structures are used in various engineering applications like aerospace, marine, automotive and so many others. The high strength and stiffness properties along with low weight, good corrosion resistance, enhanced fatigue life and low thermal expansion are the most well-known characteristics of composite materials. Many researches have been conducted on beams, plates and shells with composite materials and also functionally graded materials. Due to the existence of in-plane compressive force, stability of such structures is one of the major issues that should be considered in design. In some cases, due to weight optimization, designers allow the structure to withstand loads greater than the buckling load.

Therefore, the post-buckling analyses are also very important.

Buckling and post-buckling behaviors of laminated composite plates were considered by many researches in the past. Turvey and Marshall [1] and Argyris and Tenek [2] presented excellent reviews on methods investigating buckling and post-buckling behaviors of structures.

Ovesy et al. [3] presented a novel semi-energy finite strip method based on the first order shear deformation theory (FSDT) in order to examine the post-buckling solution for thin and relatively thick anti-symmetric angle-ply composite laminates subjected to uniform end-shortening. Komur et al. [4] carried out buckling analysis of a woven-glass-polyester laminated composite plate with a circular/elliptical hole, numerically. In the

analysis, finite element method (FEM) was applied to perform parametric studies on various plates.

Dawe et al. [5] employed semi-analytical finite strip method (FSM) to investigate the post-buckling behavior of composite structures under end-shortening. Wang and Dawe [6] developed a spline finite strip method on studying relatively thick composite plates using first order shear deformation plate theory (FSDT). Ovesy and his colleagues developed two versions of finite strip methods (semi-analytical and spline) based on the principle of minimum potential energy to predict nonlinear behavior of composite plates under end-shortening and pressure loading [7]. Ghannadpour [8] developed an exact finite strip method to predict the buckling behavior of symmetrically laminated composite rectangular plates and prismatic plate structures. He also developed a full analytical finite strip method to calculate the relative post-buckling stiffness of I-section and box-section struts [9, 10]. Very high accuracy analyses on the post-buckling behavior of channel section and box-section struts are carried out by Ghannadpour et al. [11, 12]. In their analysis, the new strip was developed based on the concept that it being effectively a plate. Ovesy et al. [13, 14] carried out studies based on the buckling and post-buckling analyses of moderately thick composite plates and plate structures using an exact finite strip.

It is noted that in all the research on the use of finite strip method in the buckling and post-buckling analyses of the plates, only simply supported boundary conditions should be assumed at loaded ends of the plate, and this is a serious limitation.

In other researches, Shen et al. [15-18] investigated the post-buckling analyses of composite and functionally graded plates under thermal and mechanical loads. These studies are mostly limited to the selection of simply supported boundary conditions on all edges of the plates. More recently, Ghannadpour and his colleagues [19-21] have investigated the post-buckling and progressive damage analyses of composite plates using semi-analytical methods. Also, Ghannadpour et al. [22, 23] have developed some new techniques to analyze the post-buckling and nonlinear behaviors of composite and functionally graded plates with different shapes of cutouts.

However, in some methods like spectral methods [24, 25], the mathematical polynomials are used to estimate the displacement fields. These polynomials allow one to analyze the plates with a

combination of different boundary conditions on all edges. Chebyshev polynomials are one category of these powerful mathematical polynomials with useful properties that can help to predict the plate behavior.

For the first time, Alwar and Nath [26] used Chebyshev polynomials to solve equilibrium equations and obtain the nonlinear behavior of isotropic circular plates. He obtained the solution to the differential equation as a sum of the Chebyshev polynomials. Nath and Kumar [27] extended this method to the rectangular domain based on classical plate theory. In circular domain, univariate Chebyshev polynomials could be used to solve equilibrium equations but for rectangular domain, bivariate Chebyshev polynomials are necessary. Shukla and Nath [28] have studied large deflection of moderately thick composite plates with different lay-up and various boundary conditions. Ghannadpour and Barekati [29] investigated initial imperfection effects on post-buckling response of laminated plates under end-shortening strain using Chebyshev techniques.

In the present paper, post-buckling behavior of thin laminated composite plates subjected to uniform in-plane end-shortening strain, is analyzed using double Chebyshev polynomials series. The mathematical formulation is based on the classical laminated plate theory and the Von-Karman assumptions. The nonlinear equations are linearized by quadratic extrapolation technique and are solved iteratively. The boundary conditions consisting of clamped, simply supported and their combinations are considered. The effects of different boundary conditions and various lay-up configurations on post-buckling response of rectangular plates are discussed extensively.

Formulation

Figure 1 shows a typical rectangular flat plate in an arbitrary coordinate. The plate is made out of laminated composite material. Classical laminated plate theory (CLPT) is used to form the equilibrium equations of plates.

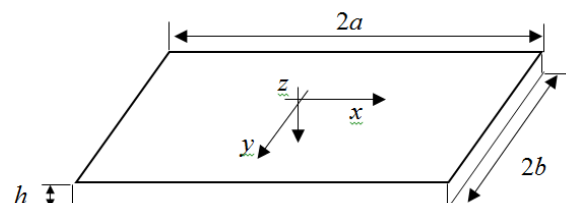


Figure 1. A typical rectangular flat plate

These equations are shown as [29]

$$\begin{aligned} \frac{\partial N_{xx}}{\partial x} + \frac{\partial N_{xy}}{\partial y} &= 0 \\ \frac{\partial N_{xy}}{\partial x} + \frac{\partial N_{yy}}{\partial y} &= 0 \\ \frac{\partial^2 M_{xx}}{\partial x^2} + 2 \frac{\partial^2 M_{xy}}{\partial x \partial y} + \frac{\partial^2 M_{yy}}{\partial y^2} + x(w_0) &= 0 \end{aligned} \quad (1)$$

Where M and N are the resultant forces and moments, respectively and $x(w_0)$ is defined as [29]:

$$\begin{aligned} N(w_0) = \frac{\partial}{\partial x} \left(N_{xx} \frac{\partial w_0}{\partial x} + N_{xy} \frac{\partial w_0}{\partial y} \right) \\ + \frac{\partial}{\partial y} \left(N_{xy} \frac{\partial w_0}{\partial x} + N_{yy} \frac{\partial w_0}{\partial y} \right) \end{aligned}$$

To solve the above equations, the displacement fields based on CLPT are defined as:

$$\begin{aligned} \bar{u}(x, y, z) &= u(x, y) - z \frac{\partial w(x, y)}{\partial x} \\ \bar{v}(x, y, z) &= v(x, y) - z \frac{\partial w(x, y)}{\partial y} \\ \bar{w}(x, y, z) &= w(x, y) \end{aligned} \quad (2)$$

Where \bar{u} , \bar{v} , and \bar{w} are components of displacement in the x , y and z directions at a general point, respectively, whilst u , v , and w are defined in the middle surface of the plates ($z=0$).

The substitution of the displacement fields, Equation (2), in the Green's expression for nonlinear strains with usual Von-Karman assumptions leads to the three strain components as [29]:

$$\begin{aligned} \begin{Bmatrix} \varepsilon_{xx} \\ \varepsilon_{yy} \\ \gamma_{xy} \end{Bmatrix} &= \begin{Bmatrix} \frac{\partial u}{\partial x} + \frac{1}{2} \left(\frac{\partial w}{\partial x} \right)^2 \\ \frac{\partial v}{\partial y} + \frac{1}{2} \left(\frac{\partial w}{\partial y} \right)^2 \\ \frac{\partial u}{\partial y} + \frac{\partial v}{\partial x} + \left(\frac{\partial w}{\partial x} \frac{\partial w}{\partial y} \right) \end{Bmatrix} + \\ z \begin{Bmatrix} -\frac{\partial^2 w}{\partial x^2} \\ -\frac{\partial^2 w}{\partial y^2} \\ -2 \frac{\partial^2 w}{\partial x \partial y} \end{Bmatrix} \end{aligned} \quad (3)$$

Where ε_x and ε_y are axial strains and γ_{xy} is shear strain.

With usual assumptions, the stress-strain relationship at a general point in CLPT formulations, for a laminated plate composed of bonded layers of unidirectional composite materials is given as:

$$\begin{Bmatrix} \sigma_{xx} \\ \sigma_{yy} \\ \tau_{xy} \end{Bmatrix} = \begin{bmatrix} \bar{Q}_{11} & \bar{Q}_{12} & \bar{Q}_{16} \\ \bar{Q}_{12} & \bar{Q}_{22} & \bar{Q}_{26} \\ \bar{Q}_{16} & \bar{Q}_{26} & \bar{Q}_{66} \end{bmatrix} \begin{Bmatrix} \varepsilon_{xx} \\ \varepsilon_{yy} \\ \gamma_{xy} \end{Bmatrix} \quad (4)$$

Where \bar{Q}_{ij} ($i, j = 1, 2, 6$) are transformed reduced stiffness coefficients.

By integrating the strain components in the thickness direction, the resultant forces and moments are obtained as:

$$\begin{aligned} \begin{Bmatrix} N_{xx} \\ N_{yy} \\ N_{xy} \end{Bmatrix} &= \int_{-h/2}^{h/2} \begin{Bmatrix} \sigma_{xx} \\ \sigma_{yy} \\ \tau_{xy} \end{Bmatrix} dz \\ \begin{Bmatrix} M_{xx} \\ M_{yy} \\ M_{xy} \end{Bmatrix} &= \int_{-h/2}^{h/2} z \begin{Bmatrix} \sigma_{xx} \\ \sigma_{yy} \\ \tau_{xy} \end{Bmatrix} dz \end{aligned} \quad (5)$$

With regard to the presented equations, the relation between the resultant forces and moments and the strains and curvatures can be expressed as:

$$\begin{aligned} \begin{Bmatrix} N_{xx} \\ N_{yy} \\ N_{xy} \end{Bmatrix} &= \begin{bmatrix} A_{11} & A_{12} & A_{16} \\ A_{21} & A_{22} & A_{26} \\ A_{16} & A_{26} & A_{66} \end{bmatrix} \begin{Bmatrix} \varepsilon_{xx}^0 \\ \varepsilon_{yy}^0 \\ \gamma_{xy}^0 \end{Bmatrix} \\ &+ \begin{bmatrix} B_{11} & B_{12} & B_{16} \\ B_{12} & B_{22} & B_{26} \\ B_{16} & B_{26} & B_{66} \end{bmatrix} \begin{Bmatrix} \varepsilon_{xx}^1 \\ \varepsilon_{yy}^1 \\ \gamma_{xy}^1 \end{Bmatrix} \begin{Bmatrix} M_{xx} \\ M_{yy} \\ M_{xy} \end{Bmatrix} \\ &= \begin{bmatrix} B_{11} & B_{12} & B_{16} \\ B_{12} & B_{22} & B_{26} \\ B_{16} & B_{26} & B_{66} \end{bmatrix} \begin{Bmatrix} \varepsilon_{xx}^0 \\ \varepsilon_{yy}^0 \\ \gamma_{xy}^0 \end{Bmatrix} \\ &+ \begin{bmatrix} D_{11} & D_{12} & D_{16} \\ D_{12} & D_{22} & D_{26} \\ D_{16} & D_{26} & D_{66} \end{bmatrix} \begin{Bmatrix} \varepsilon_{xx}^1 \\ \varepsilon_{yy}^1 \\ \gamma_{xy}^1 \end{Bmatrix} \end{aligned} \quad (6)$$

Where A is called extensional stiffness matrix, D is the bending stiffness matrix and B is called the bending-extensional coupling stiffness matrix, which are defined in terms of the lamina stiffnesses $\bar{Q}_{ij}^{(k)}$ as [30]:

$$\begin{aligned} & (A_{ij}, B_{ij}, D_{ij}) \\ & = \int_{-h/2}^{h/2} \bar{Q}_{ij}(1, z, z^2) dz \end{aligned} \quad (7)$$

Using Equations (3) to (7), the equilibrium equations can be expressed as:

$$\begin{aligned} & A_{11} \left(\frac{\partial^2 u}{\partial x^2} + \left(\frac{\partial w}{\partial x} \right) \left(\frac{\partial^2 w}{\partial x^2} \right) \right) + \\ & A_{12} \left(\frac{\partial^2 v}{\partial x \partial y} + \left(\frac{\partial w}{\partial y} \right) \left(\frac{\partial^2 w}{\partial x \partial y} \right) \right) - \\ & B_{11} \left(\frac{\partial^3 w}{\partial x^3} \right) - 2B_{16} \left(\frac{\partial^3 w}{\partial x^2 \partial y} \right) + \end{aligned} \quad (8)$$

$$\begin{aligned} & A_{66} \left(\frac{\partial^2 u}{\partial y^2} + \frac{\partial^2 v}{\partial x \partial y} + \left(\frac{\partial w}{\partial y} \right) \left(\frac{\partial^2 w}{\partial x \partial y} \right) + \right. \\ & \left. \left(\frac{\partial w}{\partial x} \right) \left(\frac{\partial^2 w}{\partial y^2} \right) \right) - B_{16} \left(\frac{\partial^3 w}{\partial x^2 \partial y} \right) - \\ & B_{26} \left(\frac{\partial^3 w}{\partial y^3} \right) = 0 \\ & A_{12} \left(\frac{\partial^2 u}{\partial x \partial y} + \left(\frac{\partial w}{\partial x} \right) \left(\frac{\partial^2 w}{\partial x \partial y} \right) \right) + \\ & A_{22} \left(\frac{\partial^2 v}{\partial y^2} + \left(\frac{\partial w}{\partial y} \right) \left(\frac{\partial^2 w}{\partial y^2} \right) \right) - \\ & B_{22} \left(\frac{\partial^3 w}{\partial y^3} \right) - 2B_{26} \left(\frac{\partial^3 w}{\partial x \partial y^2} \right) + \end{aligned} \quad (9)$$

$$\begin{aligned} & A_{66} \left(\frac{\partial^2 u}{\partial x \partial y} + \frac{\partial^2 v}{\partial x^2} + \left(\frac{\partial w}{\partial x} \right) \left(\frac{\partial^2 w}{\partial x \partial y} \right) + \right. \\ & \left. \left(\frac{\partial w}{\partial y} \right) \left(\frac{\partial^2 w}{\partial x^2} \right) \right) - B_{16} \left(\frac{\partial^3 w}{\partial x^3} \right) - \\ & B_{26} \left(\frac{\partial^3 w}{\partial x \partial y^2} \right) = 0 \\ & B_{11} \left(\frac{\partial^3 u}{\partial x^3} + \left(\frac{\partial w}{\partial x} \right) \left(\frac{\partial^3 w}{\partial x^3} \right) + \right. \\ & \left. \left(\frac{\partial^2 w}{\partial x^2} \right) \left(\frac{\partial^2 w}{\partial x^2} \right) \right) + B_{16} \left(\frac{\partial^3 u}{\partial x^2 \partial y} + \right. \\ & \left. \frac{\partial^3 v}{\partial x^3} + \left(\frac{\partial w}{\partial y} \right) \left(\frac{\partial^3 w}{\partial x^3} \right) + \right. \\ & \left. 2 \left(\frac{\partial^2 w}{\partial x^2} \right) \left(\frac{\partial^2 w}{\partial x \partial y} \right) + \right. \\ & \left. \left(\frac{\partial w}{\partial x} \right) \left(\frac{\partial^3 w}{\partial x^2 \partial y} \right) \right) + 2B_{16} \left(\frac{\partial^3 u}{\partial x^2 \partial y} + \right. \\ & \left. \left(\frac{\partial^2 w}{\partial x^2} \right) \left(\frac{\partial^2 w}{\partial x \partial y} \right) + \left(\frac{\partial w}{\partial x} \right) \left(\frac{\partial^3 w}{\partial x^2 \partial y} \right) \right) + \end{aligned} \quad (10)$$

$$\begin{aligned} & \left(\frac{\partial^2 w}{\partial x^2} \right) \left(\frac{\partial^2 w}{\partial x \partial y} \right) + \left(\frac{\partial w}{\partial x} \right) \left(\frac{\partial^3 w}{\partial x^2 \partial y} \right) \right) + \\ & 2B_{26} \left(\frac{\partial^3 v}{\partial x \partial y^2} + \left(\frac{\partial^2 w}{\partial y^2} \right) \left(\frac{\partial^2 w}{\partial x \partial y} \right) + \right. \\ & \left. \left(\frac{\partial w}{\partial y} \right) \left(\frac{\partial^3 w}{\partial x \partial y^2} \right) \right) + B_{22} \left(\frac{\partial^3 v}{\partial y^3} + \right. \\ & \left. \left(\frac{\partial w}{\partial y} \right) \left(\frac{\partial^3 w}{\partial y^3} \right) + \left(\frac{\partial^2 w}{\partial y^2} \right) \left(\frac{\partial^2 w}{\partial y^2} \right) \right) + \end{aligned}$$

$$\begin{aligned} & B_{26} \left(\frac{\partial^3 v}{\partial x \partial y^2} + \frac{\partial^3 u}{\partial y^3} + \left(\frac{\partial w}{\partial x} \right) \left(\frac{\partial^3 w}{\partial y^3} \right) + \right. \\ & \left. 2 \left(\frac{\partial^2 w}{\partial y^2} \right) \left(\frac{\partial^2 w}{\partial x \partial y} \right) + \right. \\ & \left. \left(\frac{\partial w}{\partial y} \right) \left(\frac{\partial^3 w}{\partial x \partial y^2} \right) \right) - D_{11} \frac{\partial^4 w}{\partial x^4} - \\ & D_{22} \frac{\partial^4 w}{\partial y^4} - 2(D_{12} + \\ & 2D_{66}) \frac{\partial^4 w}{\partial x^2 \partial y^2} + N(w_0) = 0 \end{aligned}$$

Method of Solution

In order to model the nonlinear response of a plate under end-shortening, the displacement fields are estimated by finite Chebyshev polynomials. These polynomials are one of the powerful mathematical series the properties of which are completely discussed in ref. [31]. To solve the equilibrium equations for composite plates with arbitrary boundary conditions, the equations must be discretized with these polynomials. This can be done through the following procedure.

If function, $\phi(x, y)$ is assumed to be a general function, it can be approximated by finite Chebyshev polynomials as:

$$\phi(x, y) = \sum_{i=0}^M \sum_{j=0}^N \delta_{ij} \phi_{ij} T_i(x) T_j(y) \quad (11)$$

Where

$$\delta_{ij} = \begin{cases} \frac{1}{4} & \text{if } i \text{ and } j = 0 \\ \frac{1}{2} & \text{if } i \text{ or } j = 0 \\ 1 & \text{otherwise} \end{cases}$$

The spatial derivatives of a general function $\phi(x, y)$ can be expressed as:

$$\begin{aligned} & \phi(x, y)_{x^r y^s} \\ & = \sum_{i=0}^{M-r} \sum_{j=0}^{N-s} \delta_{ij} (\phi_{ij})^{rs} T_i(x) T_j(y) \end{aligned} \quad (12)$$

Where, s is order of derivatives with respect to x and y respectively and the derivative function $(\phi_{ij})^{rs}$ is evaluated using the recurrence Equation (13) as [29, 32]:

$$\begin{aligned} & (\phi_{(i-1)j})^{rs} = (\phi_{(i+1)j})^{rs} \\ & + 2i(\phi_{ij})^{(r-1)s} \end{aligned} \quad (13)$$

$$(\phi_{i(j-1)})^{rs} = (\phi_{i(j+1)})^{rs} + 2j(\phi_{ij})^{r(s-1)}$$

Due to the product of variables, nonlinear terms appear in the governing equations at each step. To linearize the nonlinear terms, quadratic extrapolation technique is used at each step. A typical nonlinear term F at step k is expressed as:

$$\begin{aligned} F_k &= \sum_{i=0}^M \sum_{j=0}^N \delta_{ij} (\phi_{ij})_k T_i(x) T_j(y) \\ &= \left(\sum_{i=0}^{M-r} \sum_{j=0}^N \delta_{ij} \phi_{ij}^r T_i(x) T_j(y) \right)_k \\ &\quad \times \left(\sum_{i=0}^M \sum_{j=0}^{N-s} \delta_{ij} \phi_{ij}^s T_i(x) T_j(y) \right)_k \end{aligned} \quad (14)$$

Where

$$(\phi_{ij})_k = t_1(\phi_{ij})_{k-1} + t_2(\phi_{ij})_{k-2} + t_3(\phi_{ij})_{k-3}$$

During the analysis, the coefficient t_1 , t_2 and t_3 of the extrapolation scheme of linearization take the following values:

$$\begin{aligned} 1, 0, 0 \quad (k=1); \quad 2, -1, 0 \quad (k=2); \quad 3, -3, 1 \quad (k \geq 3) \end{aligned} \quad (15)$$

and, from [29,33], it has been shown that the product of two bivariate Chebyshev polynomials is equal to:

$$\begin{aligned} &T_i(x) T_j(y) T_k(x) T_l(y) \\ &= (1/4) [T_{i+k}(x) T_{j+l}(y) \\ &\quad + T_{i+k}(x) T_{j-l}(y) + T_{i-k}(x) T_{j+l}(y) \\ &\quad + T_{i-k}(x) T_{j-l}(y)] \end{aligned} \quad (16)$$

With regard to the above described procedure, the displacement fields could be defined by Equation (11) as:

$$\begin{aligned} u(x, y) &= -\varepsilon x + \sum_{i=0}^M \sum_{j=0}^N \delta_{ij} u_{ij} T_i(x) T_j(y) \end{aligned} \quad (17)$$

$$\begin{aligned} v(x, y) &= \alpha \varepsilon y + \sum_{i=0}^M \sum_{j=0}^N \delta_{ij} v_{ij} T_i(x) T_j(y) \end{aligned} \quad (18)$$

$$w(x, y) = \sum_{i=0}^M \sum_{j=0}^N \delta_{ij} w_{ij} T_i(x) T_j(y) \quad (19)$$

Where u_{ij} , v_{ij} and w_{ij} are the unknown Chebyshev polynomial coefficients that should be found, ε is the applied end-shortening strain and α is a constant. The term $\alpha \varepsilon y$ can show precisely the response of flat unbuckled plate to uniform end compression so that a trivial primary equilibrium path is invoked without involving any unprescribed degrees of freedom. In other words, constant α is a symbol of Poisson's effect, if unloaded edges are completely restricted from expansion $\alpha = 0$, and if the plate ends are allowed free to expand laterally; then, $\alpha = \nu$ for isotropic plates and $\alpha = A_{12}/A_{22}$ for laminated composite plates. Using Equations (12) to (16) and substituting the displacement fields into Equations (8) to (10), the nonlinear differential equations are linearized and discretized. Therefore, all of equilibrium equations and also boundary conditions are obtained in terms of the unknown Chebyshev polynomial coefficients.

After rearranging the system of equations, it can be observed that the total number of equations is more than the required coefficients. To obtain a unique solution, the least squares technique is used. In the present study, in order to obtain the accurate results, the convergence criterion is defined based on the vector containing the unknown Chebyshev polynomial coefficients (d_i). The iterative procedure is repeated until it is satisfied by:

$$\sqrt{\sum \Delta d_i^2 / \sum d_{i+1}^2} < error \quad (20)$$

Once the global equilibrium equations are solved and the unknown Chebyshev polynomial coefficients are found for a particular prescribed end-shortening, it is possible to calculate the displacements at any point in the plate using Equations (17) to (19) and to determine force and moment quantities through use of Equation (6). In

particular, the average longitudinal force N_{av} is determined by considering the membrane stress resultant N_{xx} and integrating it over the plate to give the longitudinal force acting on a plate:

$$N_{av} = \frac{\int_{-a}^a \int_{-b}^b N_{xx}(x, y) dx dy}{2a} \quad (21)$$

Results and Discussion

This section presents a number of numerical examples showing the excellent performance of the proposed algorithm, which was implemented in a MATLAB 2012b computer program. It is noted that the program is run on a standard core i5 3.1GHz PC. The results of the developed current analysis are compared with some other results which are obtained from FEM analyses carried out by the authors and FSM analysis mentioned in references. It was observed that the solution time in the presented method is about 10 percent less than those obtained by the finite element method. In order to verify the proposed method, some representative plates with various boundary conditions are considered. It is worth nothing that the error mentioned in convergence criterion (equation (20)), is taken to be 5×10^{-4} for all examples.

To establish the accuracy and stability of the method, the convergence study is performed for a square isotropic plate. The Poisson's ratio of the plate material is taken to be $\nu = 1/3$, and $2a/h = 120$. The plate is simply supported for out-of-plane behavior on all edges. In the plane of the plate, lateral expansion of the loaded ends is allowed. Furthermore, the unloaded edges are free to have lateral expansion. Convergence study for this case is shown in Figure 2. The given percentage error in figure is with respect to the solution corresponding to use of 13 Chebyshev polynomials in both directions x and y (i.e. $M+1=N+1=13$). In Figure 2, it is also seen that for all the examples under consideration the convergence studies with regard to the number of terms have revealed that 11 terms are sufficient to obtain converged results. However, the number of 13 terms is used to ensure accurate convergence in all analyses.

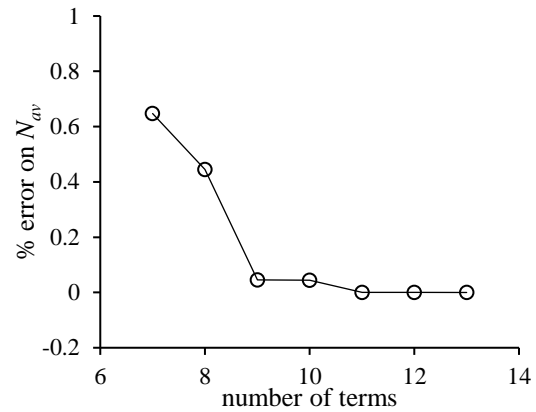


Figure 2. Convergence study with regard to the number of Chebyshev polynomials

As mentioned before, some results presented in this study have been validated by results obtained by FEM. The FEM analyses have been carried out using general purpose ABAQUS software and by using three dimensional shell element S4R. After performing convergence study, it is found that a mesh arrangement composed of 400 square elements with uniform size is required to obtain the accurate results.

Isotropic plates

In order to validate the proposed technique, isotropic plates with different boundary conditions are studied at first. Comparison is made with available results. Five different cases are studied as detailed in Table 1 with regard to the assumed conditions at their edges. To define the straight boundary condition, it is necessary to divide the displacement field v into v_0 and v_1 , as v_0 includes the terms invariant with respect to x and v_1 includes the other terms.

Table 1. End and edge conditions for five isotropic square plates

Case	In-plane displacement conditions		Out of plane displacement conditions	
	Loaded ends	Unloaded edges	Loaded ends	Unloaded edges
1	Free	Straight	S	S
2	Free	Free	S	S
3	Free	Straight	S	C
4	Held	Free	S	S
5	Held	Held	S	S

For the out-of-plane conditions, S and C denote simply supported and clamped ends or edges, respectively. For in-plane displacement conditions at loaded ends, Free and Held denote

whether the ends are free to expand laterally or held against the expansion. At unloaded edges, Free denotes that the edges are free to move laterally, i.e. are free to wave, Straight means that the edges can move laterally but remain straight and Held denotes that the edges are restricted from any lateral movement. Therefore, the mathematical models for the boundary conditions mentioned in Table 1 can be expressed as outlined in Table 2.

Table 2: The mathematical models for boundary conditions of isotropic plates

Case	In-plane displacement conditions		Out of plane displacement conditions	
	$x = \pm a$	$y = \pm b$	$x = \pm a$	$y = \pm b$
1	$u = \mp \varepsilon$ $N_{xy} = 0$	$v_1 = \int_{-a}^a N_{yy} dx$ $= N_{xy} = 0$	$w = M_{xx} = 0$	$w = M_{yy} = 0$
2	$u = \mp \varepsilon$ $N_{xy} = 0$	$N_{yy} = N_{xy} = 0$	$w = M_{xx} = 0$	$w = M_{yy} = 0$
3	$u = \mp \varepsilon$ $N_{xy} = 0$	$v_1 = \int_{-a}^a N_{yy} dx$ $= N_{xy} = 0$	$w = M_{xx} = 0$	$w = \frac{\partial w}{\partial y} = 0$
4	$u = \mp \varepsilon$ $v = 0$	$N_{yy} = N_{xy} = 0$	$w = M_{xx} = 0$	$w = M_{yy} = 0$
5	$u = \mp \varepsilon$ $v = 0$	$v = N_{xy} = 0$	$w = M_{xx} = 0$	$w = M_{yy} = 0$

Where u, v , and w are the displacement fields. To obtain the results, the Poisson's ratio ν is assumed to be 1/3 and ratio of length to thickness $2a/h = 120$. In presenting the results, the non-dimensional load is used as $F = 2N_{av}a/\pi^2 E h^3$.

Results for the five different cases are shown graphically in Figure 3, giving the non-dimensional load-end shortening variation, and in Figure 4, giving the non-dimensional load-maximum deflection variation. The values of ε_{cr} (i.e. the end shortening strain at bifurcation point) are (0.2570, 0.2570, 0.4942, 0.2375, and 0.1713) $\times 10^{-3}$ for Cases 1 to 5, respectively.

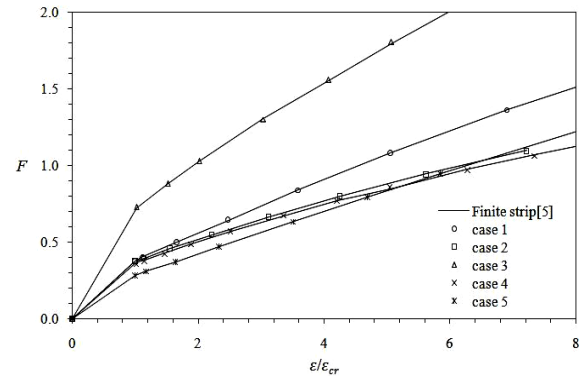


Figure 3: Longitudinal force-end shortening behavior for five isotropic plates

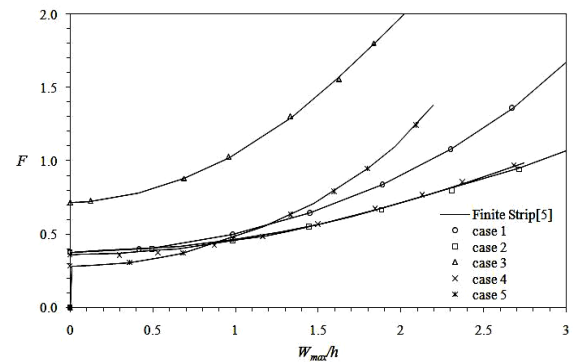


Figure 4: Longitudinal force-maximum deflection behavior for five isotropic plates

Laminated plates with simply supported ends

Anti-symmetric cross-ply

The square plates with $2a/h = 100$ and simply supported boundary condition on all edges are considered in this section. These plates have anti-symmetric cross-ply lay-up configuration as $[0/90]_{2n}$. The layers have equal thicknesses with material properties as:

$$E_1/E_2 = 40; G_{12}/E_2 = 0.5; \nu_{12} = 0.25$$

As mentioned before, all edges of the plates are simply-supported and the loaded ends are free to expand laterally in their plane. Therefore, the boundary conditions are defined as:

$$\begin{aligned} x = \pm a; u = \mp \varepsilon; w = M_x = N_{xy} = 0; \\ y = \pm b; w = M_y = N_{yy} = N_{xy} = 0; \end{aligned} \quad (22)$$

The dimensionless graphical form of results are presented in Figures 5 and 6. The Load factor used in these examples is defined as $F = N_{av}a/50E_2h^3$.

The results obtained from the present method are compared with those computed by semi-analytical finite strip method [34]. As can be seen in Figures 5 and 6, there is an excellent agreement between the results.

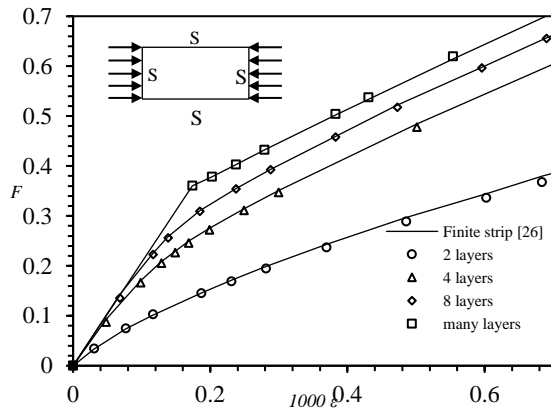


Figure 5. Longitudinal force-endshortening behavior for anti-symmetric cross-ply laminates ($2a/h = 100$)

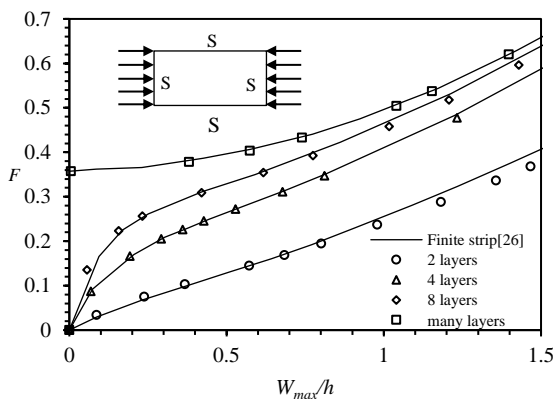


Figure 6. Longitudinal force-maximum deflection behavior for anti-symmetric cross-ply laminates ($2a/h = 100$)

It is seen that due to the presence of B_{11} and B_{22} ($B_{11} = -B_{22}$), the in-plane load causes the out of plane deflection. Hence, the bifurcation behavior will not occur since the out-of-plane displacement will take place from the onset of the application of end-shortening strain. It is also seen in figures that the increase in the number of layers significantly affects the behavior of a laminate. That is to say, a laminate with infinite number of layers, i.e. $B_{ij} = 0$, demonstrates distinctive pre-buckling and post-buckling behaviors. This is while it is difficult to pinpoint a buckling load when there is a definite number of layers.

Anti-symmetric angle-ply

In this section, anti-symmetric angle-ply laminated plates $[\pm 30]_{2n}$ with $2a/h = 100$ are considered. All the layers have equal thicknesses. Each lamina consists of composite material with the same material properties like in the previous section.

The plate boundaries are simply-supported, the loaded ends are not allowed to expand laterally and the unloaded edges are restrained against lateral expansion so that the boundary conditions can be defined as:

$$\begin{aligned} x = \pm a; u = \mp \varepsilon; w = M_x = v = \\ 0; y = \pm b; v = w = M_y = N_{xy} = 0; \end{aligned} \quad (23)$$

The history of the load-end shortening strain and load-deflection are shown in Figures 7 and 8, where the load factor is defined as same as section 4.2.1, and w_c is maximum deflection that occurs in the center of plates. The results obtained by the present method are compared with FSM results presented in [5]. As can be seen in Figures 7 and 8, there is an excellent agreement between the results. It can be seen in Figure 7 that the number of layers has a significant effect on the buckling load level but the post-buckling behavior of the various angle-ply laminates remains the same.

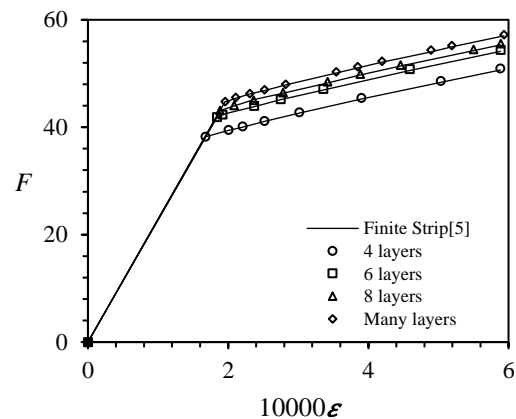


Figure 7. Longitudinal force - endshortening behavior for laminates with $[\pm 30]_{2n}$ ($2a/h = 100$)

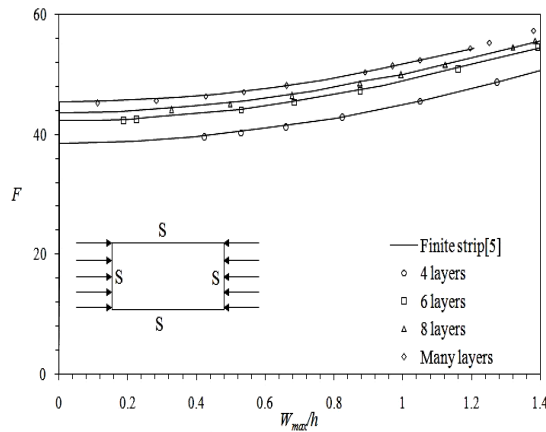


Figure 8. Longitudinal force –maximum deflection behavior of laminates with $[\pm 30]_{2n}$ ($2a/h = 100$)

As can be seen in Figures 7 and 8, the bifurcational behavior does occur when the anti-symmetric angle ply laminates are subjected to end-shortening. This happens even with the existence of the non-zero coupling coefficients B_{16} and B_{26} terms. Thus, the laminate remains flat under progressive end-shortening with uniform in-plane stiffness until the critical value.

Laminated plates with clamped ends

Three square plates (A, B, C) with clamped loaded ends and different boundary conditions along the unloaded edges are considered in this section. Loaded ends and unloaded edges are free to expand laterally in their plane. Lay-up configurations for these plates are unsymmetric cross-ply $[0/90]_2$ and the length to thickness ratio is 100. The material properties are assumed to be:

$$E_1/E_2 = 14; G_{12}/E_2 = 0.5; \nu_{12} = 0.3$$

Plate A has simply supported boundary condition along unloaded edges. Therefore, the boundary conditions for plate A are defined as:

$$\begin{aligned} x = \pm a; u = \mp \varepsilon; w = \frac{\partial w}{\partial x} = N_{xy} = 0 \\ y = \pm b; w = M_{yy} = N_{yy} = N_{xy} = 0 \end{aligned} \quad (24)$$

The out-of-plane deflection of plate A in both y and x directions is depicted in Figures 9 and 10 for a prescribed end-shortening strain $\varepsilon = 0.001$, respectively. As it can be seen, these figures also show the effect of increasing terms in the assumed displacement fields.

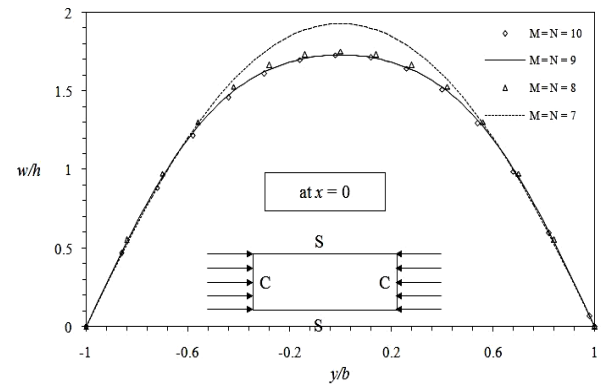


Figure 9. Out-of-plane deflection shape for plate A along y direction

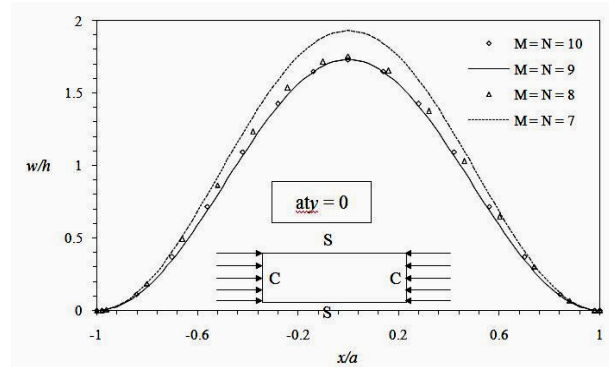


Figure 10. Out-of-plane deflection shape for plate A along x direction

As mentioned before, the in-plane displacement conditions for three plates are the same. However, the out-of-plane boundary conditions are quite different. Plate B has two clamped unloaded edges while the clamped condition is on one edge of plate C. The mathematical modeling of out-of-plane boundary conditions for the two plates, B and C, is demonstrated below:

Plate B

$$\begin{aligned} w|_{x=\pm a} = w|_{y=\pm b} = 0 \\ \frac{\partial w}{\partial x}|_{x=\pm a} = \frac{\partial w}{\partial y}|_{y=\pm b} = 0 \end{aligned} \quad (25)$$

Plate C

$$\begin{aligned} w|_{x=\pm a} = w|_{y=\pm b} = 0 \\ \frac{\partial w}{\partial x}|_{x=\pm a} = \frac{\partial w}{\partial y}|_{y=\pm b} = M_y|_{y=\pm b} = 0 \end{aligned} \quad (26)$$

The results are presented in terms of dimensionless displacements and longitudinal load in Figures 11 to 12. It may be observed from these

figures that the unsymmetrical cross ply plates with clamped boundary conditions on loaded ends have remained flat up to the buckling load and hence, a bifurcation point has occurred. As previously mentioned, the FEM analysis has been carried out using general purpose ABAQUS software. The three dimensional shell element (S4R) of the ABAQUS library has been used by a mesh arrangement composed of 400 square elements with uniform size. The results in Figures 11 and 12 are compared with those obtained by FEM. As can be seen in the figures, there is an excellent agreement between the results.

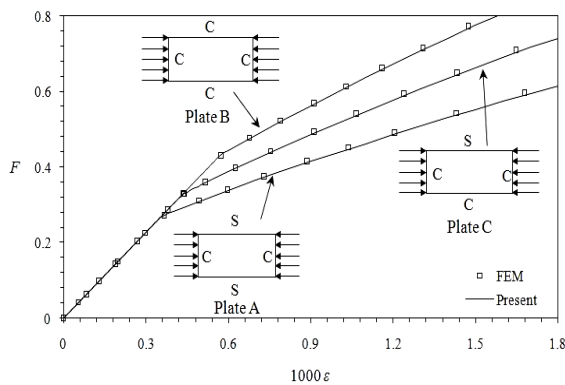


Figure 11.Effect of unloaded boundary conditions on the post-buckling behavior of unsymmetric cross-ply $[0/90]_2$

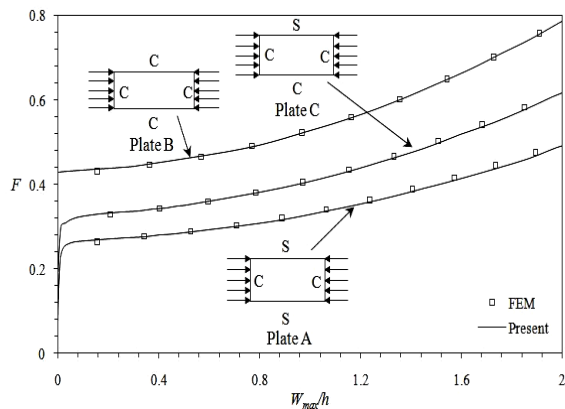


Figure 12.Post-buckling behavior of unsymmetric cross-ply $[0/90]_2$ plates with different boundary conditions

It is also worth mentioning that plate C is much more flexible than plate A due to its out-of-plane boundary conditions at unloaded edges. Therefore, as it can be seen in Figure 11, it loses more stiffness in the post-buckling regime compared with two other plates.

Such behavior can also be seen in the following figures. The out-of-plane deflection shapes for three plates, A, B and C, are depicted in Figure 13 at end-shortening strain $\epsilon = 0.001$. As it

can be seen, the plate with more clamped boundaries has a lower out-of-plane deflection.

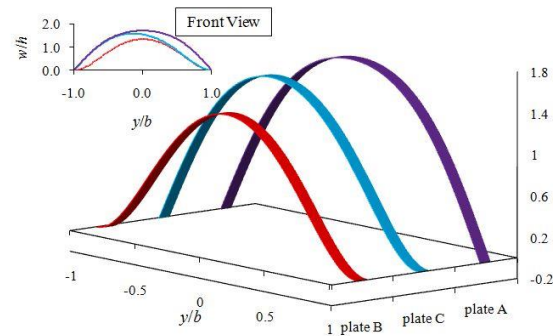


Figure 13.Non-dimensional deflection of three plates A, B and C

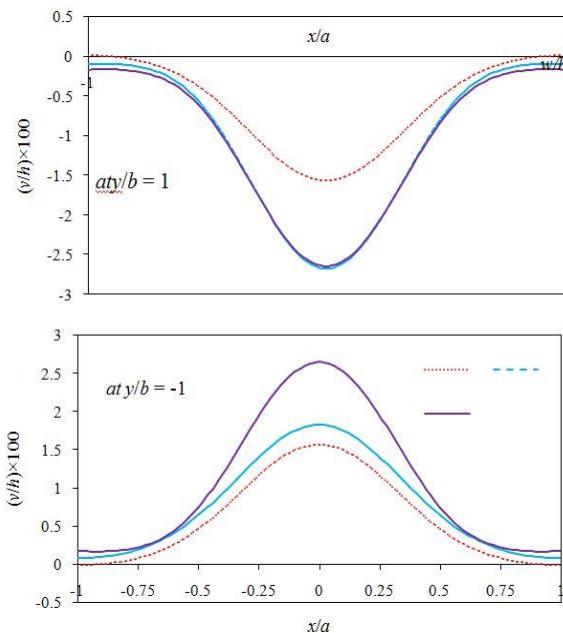


Figure 14.Lateral displacement variations(v) for three plates A, B and C

In order to investigate the lateral displacement behavior of laminated plates in post-buckling regimes, the figure shows the variation of v for three plates A, B and C. This figure also illustrates the influence of different boundary conditions on the variation of lateral displacement v . It can be seen that the non-symmetric boundary conditions create non-symmetric variation for lateral displacement on unloaded edges.

Summary

A method based on Chebyshev polynomials was developed for the examination of geometrically

nonlinear behavior of thin rectangular composite laminated plates under end-shortening strain in this study. The equilibrium equations were solved directly by substituting the displacement fields with equivalent finite double Chebyshev polynomials. The final nonlinear system of equations was obtained by discretizing both equilibrium equations and boundary conditions with finite Chebyshev polynomials. Nonlinear terms created as the product of variables were linearized by using quadratic extrapolation technique to solve the system of equations. Since the number of equations was always more than the number of unknown parameters, the least squares technique was used to solve the system of equations. The presented formulations, allow one to analyze the composite laminated plates with a combination of different boundary conditions on all edges.

References

- [1] Turvey, G.J., Marshall, I.H., *Buckling and post buckling of composite plates*. Springer Science & Business Media 1995.
- [2] Argyris, J., Tenek, L., "Recent advances in computational thermo structural analysis of composite plates and shells with strong nonlinearities." *Appl. Mech. Rev.*, 1997,50(5): 285-306.
- [3] Ovesy, H.R., Hajikazemi, M., Assaeeb, H., "A novel semi energy finite strip method for post-buckling analysis of relatively thick anti-symmetric laminated plates." *AdcEngSoftw*, 2012,48, 32-39.
- [4] Komur, M.A., Sen, F., Ataş, A., "Buckling analysis of laminated composite plates with an elliptical/circular cutout using FEM." *AdcEngSoftw*, 2010,41(2): 161-164.
- [5] Dawe, D.J., Lam, S.S.E., Azizian, Z.G., "Non-linear finite strip analysis of rectangular laminates under end shortening using classical plate theory." *Int J Numer Meth Eng*, 1992,35(5): 1087-1110.
- [6] Wang, S., Dawe, D.J., "Spline FSM postbuckling analysis of shear deformable rectangular laminates." *Thin Wall Struct*, 1999,34(2): 163-178.
- [7] Ovesy, H.R., Ghannadpour, S.A.M., Morada, G., "Post-buckling behavior of composite laminated plates under end shortening and pressure loading using two versions of finite strip method." *Compos Struct*, 2006,75(1): 106-113.
- [8] Ghannadpour, S.A.M., Ovesy, H.R., "The application of an exact finite strip to the buckling of symmetrically laminated composite rectangular plates and prismatic plate structures." *Compos Struct*, 2009,89(1): 151-158.
- [9] Ghannadpour, S.A.M., Ovesy, H.R., "An exact finite strip for the calculation of relative post-buckling stiffness of I-section struts." *Int J MechSci*, 2008,50(9): 1354-1364.
- [10] Ghannadpour, S.A.M., Ovesy, H.R., "Exact post-buckling stiffness calculation of box section struts." *Eng Computation*, 2009,26(7): 868-893.
- [11] Ghannadpour, S.A.M., Ovesy, H.R., Nassirnia, M., "High accuracy postbuckling analysis of box section struts." *Journal of Applied Mathematics and Mechanics Zeitschrift Angewandte Mathematik und Mechanik*, 2012,92(8): 668-680.
- [12] Ghannadpour, S.A.M., Ovesy, H.R., "High accuracy postbuckling analysis of channel section struts." *Int J Nonlinear Mech*, 2012,47(9): 968-974.
- [13] Ovesy, H.R., Ghannadpour, S.A.M., Zia-Dehkordi, E., "Buckling Analysis of Moderately Thick Composite Plates and Plate Structures Using an Exact Finite Strip." *Compos Struct*, 2013,95, 697-704.
- [14] Ghannadpour, S.A.M., Ovesy, H.R., Zia-Dehkordi, E., "An exact finite strip for the calculation of initial post-buckling stiffness of shear-deformable composite laminated plates." *Compos Struct*, 2014,108, 504-513.
- [15] Shen, H., Postbuckling, "analysis of orthotropic rectangular plates on nonlinear elastic foundations." *EngStruct*, 1995,17(6): 407-412.
- [16] Wang, Z.X., Shen, H.S., "Nonlinear analysis of sandwich plates with FGM face sheets resting on elastic foundations." *Compos Struct*, 2011,93(10): 2521-2532.
- [17] Shen, H.S., Zhang, C.L., "Non-linear analysis of functionally graded fiber reinforced composite laminated plates," *Part II: Numerical results*. *Int J Nonlinear Mech*, 2011,47(9): 1055-1064.
- [18] Shen, H.S., Zhu, Z.H., "Postbuckling of sandwich plates with nanotube-reinforced composite face sheets resting on elastic foundations." *European Journal of Mechanics-A/Solids* 2012,35.
- [19] Ghannadpour, S.A.M., Shakeri, M., "A New Method to Investigate the Progressive Damage of Imperfect Composite Plates Under In-Plane Compressive Load." *AUT J. Mech. Eng.* 2017, 1(2): 159-168.
- [20] Ghannadpour, S.A.M., Shakeri, M., "Energy based collocation method to predict progressive damage behavior of imperfect composite plates under compression." *Lat. Am. J. Solids Struct.*, 2018, 15(4): 1-25.
- [21] Ghannadpour, S.A.M., Barvaj, A.K., Tornabene, F., "A semi-analytical investigation on geometric nonlinear and progressive damage behavior of relatively thick laminated plates under lateral pressure and end-shortening." *Comp. Struct.* 2018, 194: 598-610.
- [22] Ghannadpour, S.A.M., Mehrparvar, M., "Energy effect removal technique to model circular/elliptical holes in relatively thick composite plates under in-plane compressive load." *Comp. Struct.* 2018, doi.org/10.1016/j.compstruct.2018.05.026.
- [23] Mehrparvar, M., Ghannadpour, S.A.M., "Plate assembly technique for nonlinear analysis of relatively thick functionally graded plates containing rectangular holes subjected to in-plane compressive load." *Comp. Struct.* 2018, doi.org/10.1016/j.compstruct.2018.04.053.
- [24] Ghannadpour, S.A.M., Kiani, P. and Reddy, J.N., "Pseudo spectral method in nonlinear analysis of relatively thick imperfect laminated plates under end-shortening strain." *Comp. Struct.* 2017, 182: 694-710.

- [25] Ghannadpour, S.A.M., Kiani, P., "Nonlinear spectral collocation analysis of imperfect functionally graded plates under end-shortening," *Struct.Eng. Mech.* 2018, 66(5): 557-568.
- [26] Alwar, R.S., Nath, Y., "Application of Chebyshev polynomials to the nonlinear analysis of circular plates," *Int J MechSci*, 1976,18(11): 589-595.
- [27] Nath, Y., Kumar, S., "Chebyshev series solution to non-linear boundary value problems in rectangular domain," *Comput Method Appl M*, 1995,125(1): 41-52.
- [28] Shukla, K.K., Nath, Y., "Nonlinear analysis of moderately thick laminated rectangular plates," *J Eng. Mech*, 2000,126(8): 831-838.
- [29] Ghannadpour, S.A.M., Barekati. B., "Initial imperfection effects on postbuckling response of laminated plates under end-shortening strain using Chebyshev techniques," *Thin-Walled Struct.* 2016,106: 484-494.
- [30] Reddy, J.N., *Mechanics of laminated composite plates and shells: theory and analysis.* CRC press 2004.
- [31] Fox, L., Parker, I.B., *Chebyshev polynomials in numerical analysis.* Oxford Univ. Press 1968.
- [32] Shukla, K.K., Nath, Y., "Analytical solution for buckling and post-buckling of angle-ply laminated plates under thermomechanical loading," *Int J NonlinearMech*, 2001,36(7): 1097-1108.
- [33] Mason, J.C. and Handscomb, D.C., *Chebyshev polynomials.* CRC Press 2002.
- [34] Ovesy, H.R., Ghannadpour, S.A.M., "Non-linear analysis of composite laminated plates under end shortening using finite strip method," *Proceedings of the fourth Australasian congress on applied mechanics*, Melbourne, Australia 2005.